

Liquid–Liquid Equilibrium Studies for Potential Solvents/Cosolvents for the Separation of Aromatics and Alkanes

Blessing Mcebo Paile, Caleb Narasigadu, and Naadhira Seedat*

Cite This: *J. Chem. Eng. Data* 2025, 70, 2422–2431

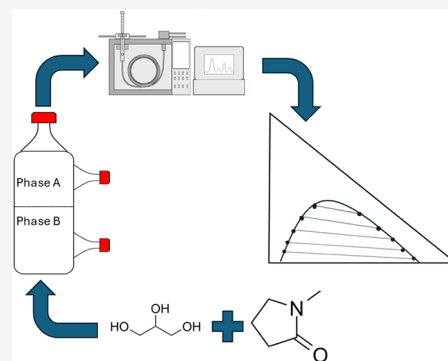
Read Online

ACCESS |

Metrics & More

Article Recommendations

ABSTRACT: Liquid–liquid equilibria (LLE) data for ternary systems of *n*-heptane + a solvent mixture + toluene were measured at 298.15 and 313.15 K and 101.3 kPa. The solvents investigated are mixtures of *N*-methylpyrrolidone and glycerol, with ratios of *N*-methylpyrrolidone to glycerol of 90:10, 70:30, and 50:50. LLE measurements were carried out using the direct analytical method, and the composition analysis was performed using gas chromatography. The effectiveness of the solvent mixtures of *N*-methylpyrrolidone and glycerol in extracting toluene from *n*-heptane was evaluated by determining the solvent selectivity and capacity and evaluating the extent of the two-phase region. All systems investigated were found to exhibit type I LLE behavior. The binodal curves were correlated to the Hlavaty β function and log γ equations. The tie-lines were correlated with the NRTL and UNIQUAC activity coefficient models. A comparison of the root-mean-square deviation (rmsd) showed that the NRTL model provided a better correlation for all systems.



1. INTRODUCTION

Aromatic compounds are essential chemicals in the petrochemical industries, and this is due to their wide range of applications in the production of several petrochemical products, which include plastics and fibers, detergents, fertilizers, explosives, pesticides, food and feed additives, nutraceuticals, and pharmaceuticals and many other important substances.^{1–4} Aromatic compounds constitute about 30% of 8 million known organic compounds; among these compounds are benzene, toluene, ethylbenzene, and xylene isomers (BTEX), which are often coproduced along other aromatic and nonaromatic compounds during petroleum refining and coal conversion.⁵ The major sources of BTEX are pyrolysis gasoline, reformer gasoline, and coke. The compositions of these sources vary for different feedstocks; typical reformer gasoline has a composition of about 25% toluene and 45% nonaromatic compounds.^{3,5} There is a need to separate BTEX from other constituents; such separation often involves aromatic and nonaromatic compounds, and the compositions usually determine the method of separation. Due to relative volatilities near unity and azeotrope formations between aromatic and aliphatic compounds, conventional separation processes like distillation are not practical. Rather, they can be separated by liquid–liquid extraction, extractive distillation, or azeotropic distillation, the composition of the aromatic compound in the mixtures often determines the type of separation applied.⁶ Liquid–liquid ionic extraction of aromatic compounds with ionic solvent has been applied for 20–65 wt % aromatic content, 65–90 wt % of aromatic content naphtha

is separated via extractive distillation, and azeotropic distillation is used to separate naphtha with aromatic content greater than 90 wt %.^{4,6} Naphtha with aromatic content lower than 20 wt % exists but is technologically challenging to separate.⁷ Extractive distillation and liquid–liquid extraction require the inclusion of a solvent to alter the relative volatility of the mixture and create partitioning, respectively. The commonly used organic solvents, which are usually polar, are sulfolane and glycols, while others include ethylene glycols dimethylformamide, *N*-formyl morpholine, and *N*-methyl pyrrolidine.⁶ Desirable characteristics of ionic liquids, such as low vapor pressure, wide liquid range, and relatively high density when compared with aromatic and aliphatic compounds, placed them as alternatives to organic solvents. Ionic liquids that have been tested include imidazolium, pyridinium, ammonium, and pyrrolidinium, which have also been employed as solvents in the extraction of aromatic compounds.⁸ The major drawback of ionic liquids as solvents for liquid–liquid extraction is the difficulty in finding ionic liquids with high selectivity, low toxicity, low viscosity, and high capacity.⁹

Received: October 27, 2024

Revised: April 15, 2025

Accepted: April 22, 2025

Published: May 5, 2025



There have been several applications of organic solvents for the extraction of aromatic compounds. Alkhaldi et al.¹⁰ represented the Kuwait middle distillate with a multi-component mixture with dodecane, hexadecane, 1,3,5-trimethylbenzene (mesitylene), and butylbenzene as its constituents, and *N*-methyl-2-pyrrolidone (NMP) was used as an organic solvent for the liquid–liquid extraction process. Sulfolane was used as a solvent for the extraction of toluene in a mixture of toluene and heptane by Meindersma et al.¹¹ DongChu et al.¹² carried out the liquid–liquid equilibrium of the ternary mixture of heptane, xylene, and *N*-formylmorpholine, this is to determine the ability of *N*-formylmorpholine to extract xylene. Mohsen-Nia et al.¹³ used each of tetramethylene sulfone, dimethyl sulfoxide (DMSO), and ethylene carbonate solvents for the extraction of toluene or *m*-xylene from its mixtures with *n*-heptane or *n*-octane or cyclohexane.

Mesquita et al.¹⁴ evaluated 2-hydroxy ethylammonium formate (2-HEAF) and glycerol as solvents for extracting toluene from decane and toluene mixtures.

The success of a solvent extraction process depends on the selection of a suitable solvent. Properties of such a solvent include a high selectivity for aromatics, high capacity, ability to form two phases at reasonable temperatures, and low risks to health, safety, and the environment (HSE).¹⁵

However, these solvents do not possess all of the properties of an ideal solvent. For instance, NMP has a very high capacity and a relatively low selectivity.¹⁶ The combination of solvents can overcome such cases.¹⁷

In a solvent screening methodology, Brijmohan et al.,¹⁸ identified glycerol as a potential solvent in aromatics recovery. However, the use of glycerol is accompanied by a low-performance index due to low solvent capacities.¹⁹ To overcome this challenge and increase the degree of BTEX separation from its mixtures, exploring other solvents and the effect of cosolvents via the liquid–liquid extraction technique is pertinent. In this study, the extraction strength of glycerol and NMP was investigated in different ratios and temperatures,

glycerol was used as a cosolvent with NMP. The system under consideration is *n*-heptane + (NMP + glycerol) + toluene, and the LLE measurements were carried out at 298.15 and 313.15 K and 101.3 kPa using different NMP to glycerol mass ratios of 90:10, 70:30, and 50:50. The LLE data reported in this work serve to fill the knowledge gap pertaining to the equilibrium properties of an *n*-alkane + NMP + glycerol + aromatic system.

2. EXPERIMENTAL AND COMPUTATIONAL METHODS

2.1. Materials. Refractive index measurements ascertained the chemical purity of the chemicals used in this study. An Atago refractometer (model RX 7000i) with an overall uncertainty of 0.0001 was used.²⁰ Table 1 lists the respective chemical supplier information and refractive index measurements. The chemicals were used without further purification.

2.2. Equipment. The LLE measurements were undertaken by using the direct analytical technique. The experimental procedure employed is that of Alders.²³ Solvent mixtures were prepared by mixing the solvent (NMP) with the cosolvent (glycerol) to create mixtures with NMP to glycerol mass ratios of 90:10 (NMP + 10% glycerol), 70:30 (NMP + 30% glycerol), and 50:50 (NMP + 50% glycerol). The LLE measurements were carried out in a double-walled glass cell depicted in Figure 1c. The adoption of this cell was proposed

Table 1. Chemical Purity Analysis at 101.3 kPa

Chemical	CAS Reg. No.	Chemical supplier	Mass fraction purity ^b	Refractive Index (n_D) ^a	
				Measured ^c	Lit
Glycerol	56-81-5	Sigma-Aldrich	>0.99	1.4736	1.4730 ²¹
NMP	872-50-4	Sigma-Aldrich	>0.99	1.4689	1.4690 ²¹
Toluene	108-88-3	Glassworld	>0.99	1.4963 ^d	1.4967 ²²
<i>n</i> -Heptane	142-82-5	Sigma-Aldrich	>0.99	1.3853	1.3855 ²²

^aRefractive index at 298.15 K, $u(T) = 0.1$ K. ^bAs stated by supplier standard uncertainties are. ^c $u(n_D) = 0.0001$. ^dRefractive index at 293.15 K, $u(T) = 0.1$ K.

by Narasigadu et al.²⁴ The design of this cell allowed for temperature control by the circulation of water through the jacket of the cell. Temperature measurement with a precision of 0.1 K²⁰ was achieved by a HellermannTyton T235H multimeter sensor housed in the thermowell of the cell. The sensor was calibrated with the WIKA CTH6500 thermometer. The Nexis GC-2030 gas chromatograph with flame ionizing detector (FID) from Shimadzu Corporation was used for the composition analysis. The calibration of the detector followed the method detailed by Raal and Mühlbauer,²⁵ which employed area ratios of single-phase samples of known composition across the composition range of 0 to 1. The uncertainty in the mole fraction compositions, which may be attributed to instrument stability, sample preparation, and repeatability, was 0.006.²⁰ The column used was the SH-Rxi-5 ms from Restek with the dimensions: 30 m, 0.25 mm ID, and 0.25 μ m column thickness. The agitation and equilibrium waiting times for each measurement were 1 h each. A minimum of three 1 μ L samples were analyzed for each phase. The relative standard deviation (RSD) values for the area ratios of each phase were <2%. The computation of the RSD followed the method outlined by Box et al.²⁶ The experimental setup is illustrated in Figure 1.

2.3. Data Correlation. Empirical functions of varying complexity have been developed for the correlation of binodal curve data.^{27–31} This study employed the Hlavatý,²⁸ β function,³⁰ and $\log \gamma$ ²⁹ equations, represented by eqs 1–3, for the correlation of the binodal curve data. These models are purely mathematical and have no thermodynamic basis. In their application, these models have been found to display good precision, passing through the solubility curve on both phases and require few coefficients.³² Furthermore, the appropriate choice of independent variables for the β function and $\log \gamma$ equation avoids the problem of having highly intercorrelated variables.^{32,33} The solvent and cosolvent were treated as a pseudocomponent in the correlation of the binodal curve and tie-line data as has been done previously.³⁴

Hlavatý²⁸ equation with coefficients A_i

$$x_3 = A_1 x_A \ln x_A + A_2 x_B \ln x_B + A_3 x_A x_B \quad (1)$$

β function equation of Letcher et al.³⁰ with coefficients B_i

$$x_3 = B_1 (1 - x_A)^{B_2} x_A^{B_3} \quad (2)$$

$\log \gamma$ equation of Letcher et al.,²⁹ with coefficients C_i

$$x_3 = C_1 (-\ln x_A)^{C_2} x_A^{C_3} \quad (3)$$

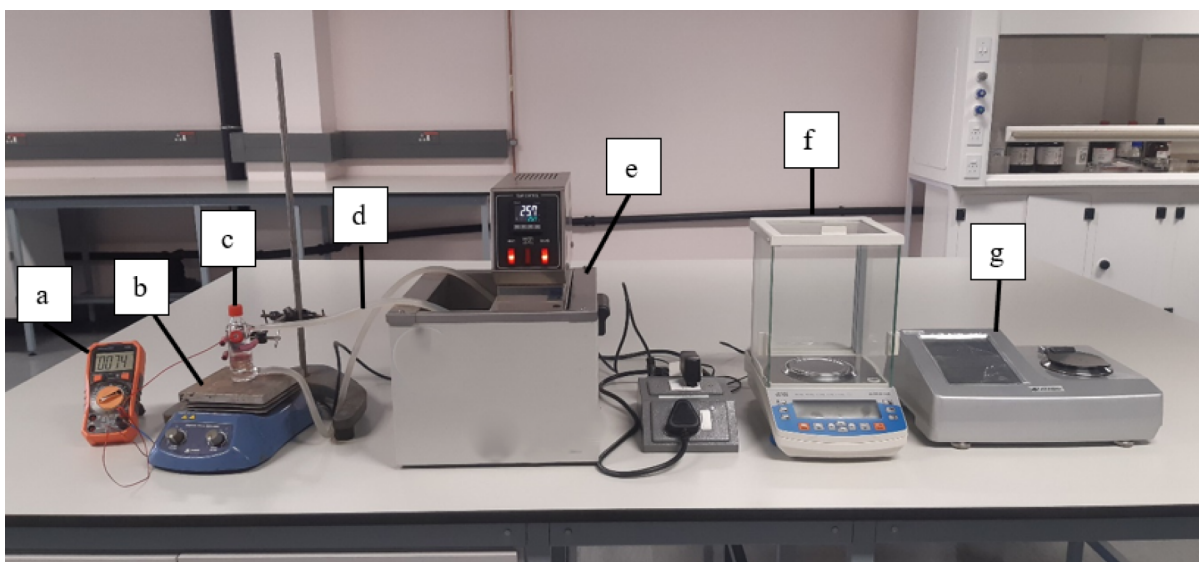


Figure 1. Experimental setup: multimeter (a), magnetic stirrer (b), equilibrium cell (c), silicon pipes (d), water bath (e), balance (f), and refractometer (g). [Image taken by one of the authors].

Table 2. Experimental LLE Data for *N*-Heptane (1) + Solvent[90% NMP (2) + 10% Glycerol (3)] + Toluene (4) System at 298.15 and 313.15 K and 101.3 kPa^a

Solvent-Rich Phase				<i>n</i> -Heptane-Rich Phase				ω	K_2
x_1	x_2	x_3	x_4	x_1	x_2	x_3	x_4		
298.15 K									
0.1369	0.7709	0.0922	0.0000	0.9027	0.0869	0.0104	0.0000	-	-
0.1395	0.7409	0.0886	0.0310	0.8313	0.1106	0.0132	0.0449	4.1143	0.6904
0.1481	0.7052	0.0844	0.0623	0.7463	0.1463	0.0175	0.0899	3.4921	0.6930
0.1635	0.6442	0.0771	0.1152	0.6151	0.2070	0.0248	0.1531	2.8307	0.7524
0.1848	0.5948	0.0711	0.1493	0.5249	0.2504	0.0300	0.1947	2.1781	0.7668
0.2304	0.5160	0.0617	0.1919	0.4347	0.3039	0.0364	0.2250	1.6092	0.8529
313.15 K									
0.1522	0.7572	0.0906	0.0000	0.8898	0.0984	0.0118	0.0000	-	-
0.1540	0.7198	0.0861	0.0401	0.8068	0.1286	0.0154	0.0492	4.2700	0.8150
0.1475	0.7034	0.0841	0.0650	0.7133	0.1601	0.0191	0.1075	2.9241	0.6047
0.1605	0.6594	0.0789	0.1012	0.6118	0.2127	0.0254	0.1501	2.5700	0.6742
0.1863	0.6031	0.0721	0.1385	0.5413	0.2451	0.0293	0.1843	2.1835	0.7515
0.2298	0.5276	0.0631	0.1795	0.4620	0.2950	0.0353	0.2077	1.7375	0.8642

^aStandard uncertainties are $u(T) = 0.1$ K; $u(x) = 0.006$.

where

$$x_A = \frac{\left(x_2 + \frac{1}{2}x_3 - x_2^0\right)}{\left(x_{22}^0 - x_2^0\right)} \quad (4)$$

$$x_B = \frac{\left(x_{22}^0 - x_2 - \frac{1}{2}x_3\right)}{\left(x_{22}^0 - x_2^0\right)} \quad (5)$$

In eqs 1–5, x_2 refers to the mole fraction composition of the solvent; x_3 refers to the mole fraction composition of toluene; and x_{22}^0 and x_2^0 represent the values of x_2 on the binodal curve that cut the $x_3 = 0$ axis. The best fit correlation was based on the lowest value of the standard deviation (σ) which is represented by eq 6:

$$\sigma = \left\{ \sum_{k=1}^n \frac{[x_3(\text{calc}) - x_3(\text{exp})]_k^2}{(n-3)} \right\}^{1/2} \quad (6)$$

where x_3 represents the mole fraction of toluene; n represents the number of data points; and 3 represents the number of estimated coefficients.³⁵ The tie-lines were correlated with the NRTL model of Renon and Prausnitz³⁶ and the UNIQUAC activity coefficient model of Anderson and Prausnitz³⁷ using ASPEN Plus software. The correlation procedure employed the Britt–Leucke algorithm,³⁸ the Deming initialization method,³⁹ and the minimization of a nonlinear least-squares objective function.⁴⁰ In the NRTL model regression, the value of the nonrandomness parameter (α_{ij}) was set to be equal for all binary pairs and fixed at either 0.20, 0.30, 0.40, or 0.48 as suggested by Walas.⁴¹ The best-fit correlation was indicated by the lowest value of the root-mean-square deviation (rmsd), computed by eq 7:

$$\text{rmsd} = \left\{ \frac{\sum_a \sum_b \sum_c (x_{abc}(\text{exp}) - x_{abc}(\text{calc}))^2}{6k} \right\}^{1/2} \quad (7)$$

Table 3. Experimental LLE Data for *N*-Heptane (1) + Solvent[70%NMP(2) + 30% Glycerol(3)] + Toluene (4) System at 298.15 and 313.15 K and 101.3 kPa^a

Solvent-Rich Phase				<i>n</i> -Heptane-Rich Phase				ω	K_2
x_1	x_2	x_3	x_4	x_1	x_2	x_3	x_4		
298.15 K									
0.0919	0.6214	0.2867	0.0000	0.9481	0.0355	0.0164	0.0000	-	-
0.1107	0.5866	0.2706	0.0321	0.8863	0.0458	0.0211	0.0468	5.4915	0.6859
0.1222	0.5514	0.2544	0.0720	0.7686	0.0864	0.0399	0.1051	4.3088	0.6851
0.0923	0.5383	0.2484	0.1210	0.6931	0.1005	0.0464	0.1600	5.6788	0.7563
0.1221	0.4955	0.2286	0.1538	0.5886	0.1308	0.0603	0.2203	3.3655	0.6981
0.1196	0.4634	0.2138	0.2032	0.4731	0.1727	0.0796	0.2746	2.9272	0.7400
0.1476	0.4040	0.1864	0.2620	0.3783	0.2131	0.0983	0.3103	2.1641	0.8443
313.15 K									
0.1305	0.5950	0.2745	0.0000	0.9369	0.0432	0.0199	0.0000	-	-
0.1412	0.5647	0.2605	0.0336	0.8242	0.0747	0.0344	0.0666	2.9452	0.5045
0.1378	0.5199	0.2399	0.1024	0.7040	0.1085	0.0500	0.1375	3.8047	0.7447
0.1403	0.4659	0.2150	0.1788	0.5633	0.1549	0.0714	0.2104	3.4120	0.8498
0.1647	0.4120	0.1901	0.2332	0.4570	0.1867	0.0861	0.2702	2.3948	0.8631
0.1866	0.3786	0.1746	0.2602	0.3844	0.2174	0.1003	0.2979	1.7993	0.8735

^aStandard uncertainties are $u(T) = 0.1$ K; $u(x) = 0.006$.

Table 4. Experimental LLE Data for *N*-Heptane (1) + Solvent[50%NMP (2) + 50% Glycerol (3)] + Toluene (4) System at 298.15 and 313.15 K and 101.3 kPa^a

Solvent-Rich Phase				<i>n</i> -Heptane-Rich Phase				ω	K_2
x_1	x_2	x_3	x_4	x_1	x_2	x_3	x_4		
298.15 K									
0.0767	0.4447	0.4786	0.0000	0.9750	0.0120	0.0130	0.0000	-	-
0.0668	0.4346	0.4678	0.0308	0.9275	0.0159	0.0171	0.0395	10.8266	0.7797
0.1084	0.4048	0.4357	0.0511	0.8634	0.0240	0.0259	0.0867	4.6944	0.5894
0.1324	0.3605	0.3880	0.1191	0.7762	0.0292	0.0315	0.1631	4.2810	0.7302
0.1292	0.3019	0.3250	0.2439	0.6001	0.0651	0.0701	0.2647	4.2798	0.9214
0.1453	0.2623	0.2824	0.3100	0.4814	0.0870	0.0937	0.3379	3.0396	0.9174
0.1610	0.2364	0.2545	0.3481	0.4031	0.1097	0.1181	0.3691	2.3613	0.9431
313.15 K									
0.1098	0.4287	0.4615	0.0000	0.9620	0.0183	0.0197	0.0000	-	-
0.1303	0.3855	0.4150	0.0692	0.8235	0.0315	0.0340	0.1110	3.9400	0.6234
0.1487	0.3369	0.3626	0.1518	0.7087	0.0461	0.0497	0.1955	3.7001	0.7765
0.1585	0.2984	0.3213	0.2218	0.6066	0.0659	0.0709	0.2566	3.3081	0.8644
0.1766	0.2590	0.2789	0.2855	0.4759	0.0944	0.1016	0.3281	2.3449	0.8702
0.1977	0.2317	0.2495	0.3211	0.3991	0.1152	0.1240	0.3617	1.7921	0.8878

^aStandard uncertainties are $u(T) = 0.1$ K; $u(x) = 0.006$.

where k is the number of experimental points, x is the mole fraction, and the subscripts a , b , and c represent component, phase, and tie-line, respectively.

2.4. Selectivity and Capacity. The solvent capacity, represented by the distribution coefficient (K), is a measure of the solvent power, it indicates the maximum volume of aromatics that the solvent can contain.¹⁸ Therefore, its value should preferably be high so that a low ratio of solvent to feed may be used for an effective separation.⁴² The ratio of the distribution coefficient of the aromatics and nonaromatics yields the selectivity (ω) of the solvent. In the present work, the selectivity measures the ability of the solvent to separate toluene from *n*-heptane. Thus, a value greater than unity indicates effective toluene recovery. Solvent capacity and selectivity are mathematically expressed by eqs 8 and 9, respectively:

$$K_2 = \frac{(x_3)^{II}}{(x_3)^I} \quad (8)$$

$$\omega = \frac{(x_3)^{II}/(x_3)^I}{(x_1)^{II}/(x_1)^I} \quad (9)$$

where subscripts 1, 2, and 3 represent *n*-heptane, solvent (NMP and glycerol as a pseudocomponent), and toluene, respectively. Superscripts I and II represent *n*-heptane-rich and solvent-rich phases, respectively.

A value of unity for the selectivity represents the plait point. At this point, the two phases have identical compositions; therefore, no separation can be achieved. This point was determined using the graphical Coolidge method.⁴³

3. RESULTS AND DISCUSSION

In this section, systems are referenced in terms of their solvent mixing ratios. The experimental LLE data and respective

selectivities and capacities for the systems under investigation are represented in Tables 2–4. Estimations of the plait point compositions obtained from the graphical Coolidge method are presented in Table 5. Compositions are presented in terms

Table 5. Estimated Plait Point Composition Using the Graphical Coolidge Method^{ab}

<i>T</i> (K)	<i>x</i> ₁	<i>x</i> ₂	<i>x</i> ₃	<i>x</i> ₄
<i>n</i> -heptane (1) + NMP(2) + glycerol(3) + toluene (4)				
298.1500	0.3194	0.3976	0.0475	0.2355
313.1500	0.3759	0.3582	0.0428	0.2231
<i>n</i> -heptane (1) + NMP(2) + glycerol(3) + toluene (4)				
298.1500	0.2628	0.2814	0.1298	0.3260
313.1500	0.2379	0.3045	0.1405	0.3171
<i>n</i> -heptane (1) + NMP(2) + glycerol(3) + toluene (4)				
298.1500	0.2619	0.1711	0.1841	0.3829
313.1500	0.2710	0.1757	0.1891	0.3642

^aStandard uncertainty is $u(T) = 0.1$ K. ^b*n*-heptane (1) + solvent [NMP(2) + glycerol(3)] + toluene (4) system at 298.15 and 313.15 K and 101.3 kPa.

of mole fractions where x_1 , x_2 , x_3 , and x_4 represent the mole fractions of *n*-heptane, NMP, glycerol (solvent mixtures), and toluene, respectively.

Figures 2–7 graphically present the experimental and modeled data of the best fit for the systems under

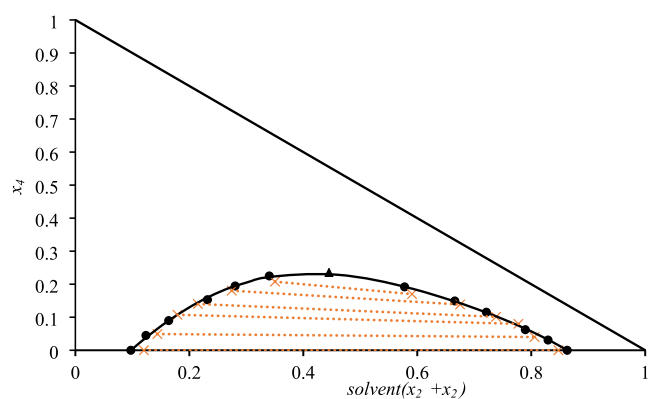


Figure 2. LLE for *n*-heptane (1) + solvent mixture [90% NMP(2) + 10% glycerol(3)] + toluene (5) system at 298.15 K and 101.3 kPa. ●, Experimental data; ▲, plait point; —, β function; ●●x●●●, NRTL ($\alpha = 0.2$).

investigation, while their Hlavatý equation, β function, log γ equation, NRTL, and UNIQUAC parameters are tabulated in Tables 6–11. As the systems are quaternary, the activity coefficient interaction parameters are presented for 4 components where 1, 2, 3, and 4 represent *n*-heptane, NMP, glycerol, and toluene, respectively. All systems produced one pair of partially miscible liquids at 298.15 and 313.15 K and 101.3 kPa. Therefore, they are classified as type I LLE systems.⁴⁴ The β function equation provided a better correlation for the binodal curves of all systems. The NRTL model provided a better correlation for the tie-lines of all systems. This can be attributed to the nonrandomness parameter (α_{ij}). Proper selection of α_{ij} makes the NRTL model applicable to a variety of mixtures, while other models appear to be limited to specific types.³⁶ In the NRTL model, favorable and unfavorable interactions between species *i* and *j*

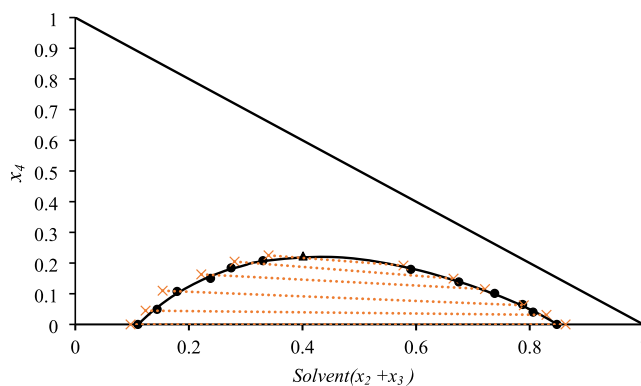


Figure 3. LLE for *n*-heptane (1) + solvent mixture [90% NMP(2) + 10% glycerol(3)] + toluene (4) system at 313.15 K and 101.3 kPa. ●, Experimental data; ▲, plait point; —, β function; ●●x●●●, NRTL ($\alpha = 0.2$).

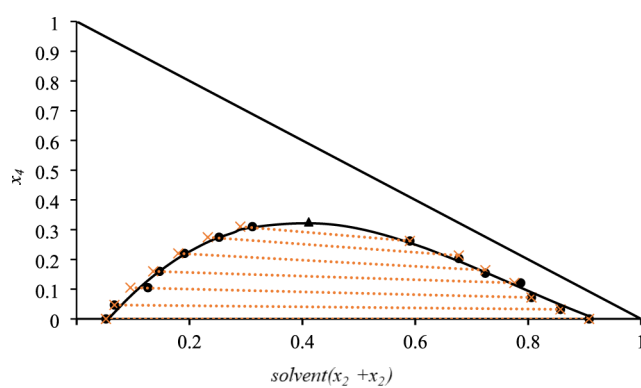


Figure 4. LLE for *n*-heptane (1) + solvent mixture [70% NMP(2) + 30% glycerol(3)] + toluene (4) system at 298.15 K and 101.3 kPa. ●, Experimental data; ▲, plait point; —, β function; ●●x●●●, NRTL ($\alpha = 0.2$).

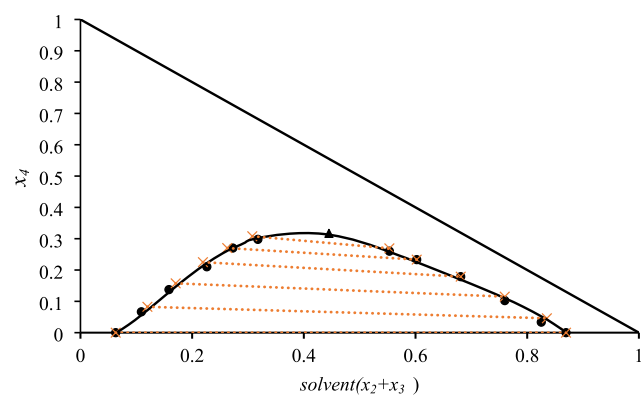


Figure 5. LLE for *n*-heptane (1) + solvent mixture [70% NMP(2) + 30% glycerol(3)] + toluene (4) system at 313.15 K and 101.3 kPa. ●, Experimental data; ▲, plait point; —, β function; ●●x●●●, NRTL ($\alpha = 0.2$).

are represented by negative and positive values of the binary interaction parameters, respectively.⁴⁵ As such, interaction parameters for the immiscible *n*-heptane and glycerol pair move from negative to positive with the increase in glycerol content and the miscible *n*-heptane and toluene pair have negative interaction parameters, as shown in Tables 9–11. Figures 2–7 show that the size of the two-phase region

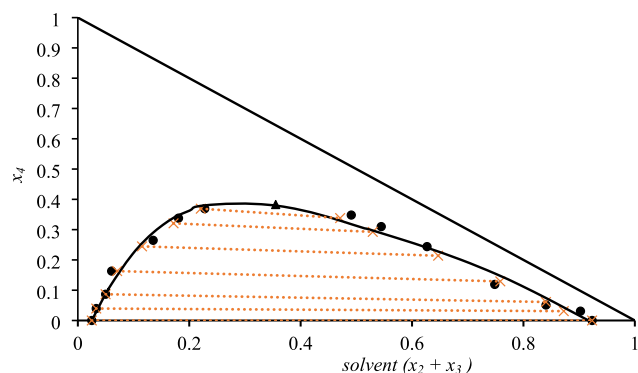


Figure 6. LLE for the *n*-heptane (1) + solvent mixture [50% NMP(2) + 50% glycerol(3)] + toluene (4) system at 298.15 K and 101.3 kPa. ●, Experimental data; ▲, plait point; —, β function; ●●x●●●, NRTL ($\alpha = 0.2$).

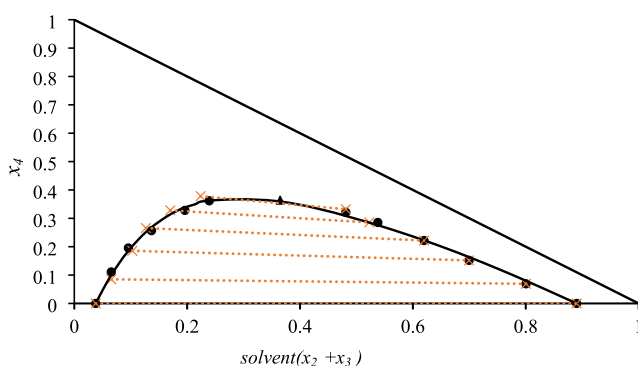


Figure 7. LLE for *n*-heptane (1) + solvent mixture [50% NMP(2) + 50% glycerol(3)] + toluene (3) system at 313.15 K and 101.3 kPa. ●, Experimental data; ▲, plait point; —, β function; ●●x●●●, NRTL ($\alpha = 0.2$).

Table 6. Binodal Curve Correlation Parameters for the *N*-Heptane (1) + (NMP + 10% Glycerol) (2) + Toluene (3) System at 298.15 and 313.15 K and 101.3 kPa

Hlavatý Equation		β Function Equation		Log γ Equation	
298.15 K					
A_1	0.3155	B_1	0.9209	C_1	0.8566
A_2	0.2377	B_2	0.8891	C_2	0.8603
A_3	1.3791	B_3	1.1376	C_3	1.4691
σ	0.0103	σ	0.0038	σ	0.0046
313.15 K					
A_1	0.3445	B_1	0.7429	C_1	0.6999
A_2	0.0016	B_2	0.7699	C_2	0.7479
A_3	1.4121	B_3	1.0207	C_3	1.3105
σ	0.0163	σ	0.0048	σ	0.0058

increased with the increase in the glycerol content of the solvent. Brijmohan et al.¹⁹ found the application of pure glycerol in aromatics recovery demonstrated type II LLE behavior⁴⁴ which is attributed to glycerol's high density.¹⁶ This translates to a large area over which the separation of toluene from *n*-heptane can occur. Therefore, this property of glycerol was intensified when the glycerol content was increased in the solvent mixtures under investigation. The size of the two-phase regions, listed in decreasing order of magnitude, is as follows: NMP + 50% glycerol > NMP + 30% glycerol > NMP + 10% glycerol. A similar trend was also observed by Naidoo et al.³⁴

Table 7. Binodal Curve Correlation Parameters for *N*-Heptane (1) + (NMP + 30% Glycerol) (2) + Toluene (3) System at 298.15 and 313.15 K and 101.3 kPa

Hlavatý Equation		β Function Equation		Log γ Equation	
298.15 K					
A_1	0.4874	B_1	1.6958	C_1	1.5698
A_2	0.0759	B_2	1.0465	C_2	1.0163
A_3	1.9507	B_3	1.3598	C_3	1.7589
σ	0.0201	σ	0.0177	σ	0.0184
313.15 K					
A_1	0.6783	B_1	1.5766	C_1	1.4751
A_2	0.1104	B_2	0.9798	C_2	0.9536
A_3	2.1675	B_3	1.4212	C_3	1.8007
σ	0.0184	σ	0.0107	σ	0.0116

Table 8. Binodal Curve Correlation Parameters for *N*-Heptane (1) + (NMP + 50% Glycerol) (2) + Toluene (3) System at 298.15 and 313.15 K and 101.3 kPa

Hlavatý Equation		β Function Equation		Log γ Equation	
298.15 K					
A_1	0.3748	B_1	2.1457	C_1	1.8906
A_2	0.2583	B_2	1.1824	C_2	1.1236
A_3	2.0964	B_3	1.2629	C_3	1.6763
σ	0.0236	σ	0.0228	σ	0.0244
313.15 K					
A_1	0.3596	B_1	1.8962	C_1	1.7109
A_2	0.1879	B_2	1.1303	C_2	1.0849
A_3	2.2379	B_3	1.2216	C_3	1.6339
σ	0.0109	σ	0.0101	σ	0.0116

Table 9. NRTL and UNIQUAC Interaction Parameters for the *N*-Heptane (1) + (NMP (2) + 10% Glycerol (3)) + Toluene (4) System at 298.15 and 313.15 K and 101.3 kPa

Component	ij	ji	NRTL Parameters ($\alpha = 0.2$)			UNIQUAC Parameters		
			$g_{ij} - g_{ji}$	$g_{ij} - g_{ii}$	rmsd	$u_{ij} - u_{ji}$	$u_{ij} - u_{ii}$	rmsd
298.15 K								
12	21		-8.588	1.544	0.0058	15.30	-1.8314	0.0423
13	31		-1.731	4.011		-0.2239	1.090	
14	41		-0.3302	5.086		-1.506	-0.8734	
23	32		50.77	827.1		-3.356	420.3	
24	42		79.16	-31.64		68.96	68.96	
34	43		1.208	12.05		0.2442	13.16	
313.15 K								
12	21		19.70	-2.372	0.0066	-222.5	3.058	0.0931
13	31		-0.7364	6.149		63.92	4.883	
14	41		-0.6616	3.740		-0.4512	-0.1915	
23	32		-4.636	75.96		-2.567	364.3	
24	42		3920	63.92		601.9	39.06	
34	43		1.361	4.023		2.240	2.405	

In Figures 8–11, the selectivity and capacity of the systems investigated are compared with those of pure NMP⁴⁶ and glycerol¹⁹ as well as the conventional solvents sulfolane⁴⁷ and NFM.⁴² Figures 8 and 9 show that the solvents under investigation showed higher or comparable selectivities with an increasing glycerol content. Furthermore, Figures 8 and 9 show that the selectivity decreases with increasing toluene content in the feed as well as with increasing temperature. This is the result of the increased miscibility between the toluene and

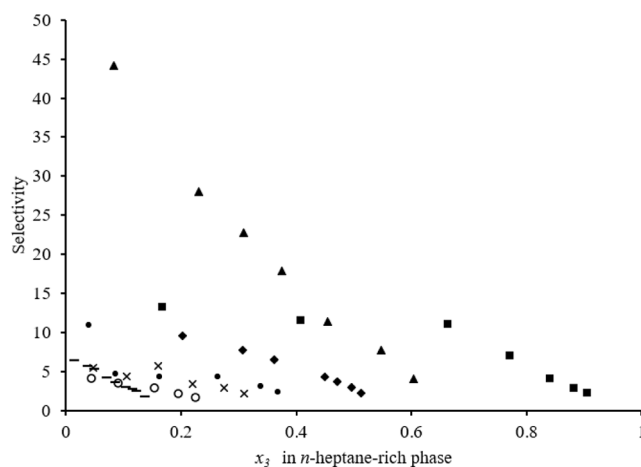
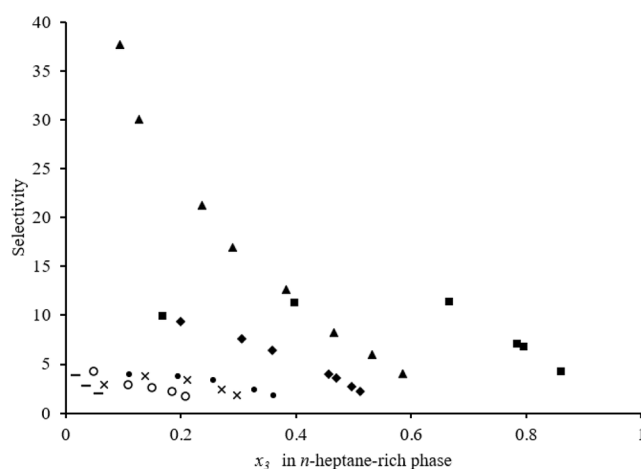
Table 10. NRTL and UNIQUAC Interaction Parameters for *N*-Heptane (1) + (NMP (2) + 30% Glycerol (3)) + Toluene (4) System at 298.15 and 313.15 K and 101.3 kPa

Component		NRTL Parameters ($\alpha = 0.2$)			UNIQUAC Parameters		
<i>ij</i>	<i>ji</i>	g_{ij} – g_{jj}	g_{ji} – g_{ii}	rmsd	u_{ij} – u_{jj}	u_{ji} – u_{ii}	rmsd
298.15 K							
12	21	–43.08	–1.205	0.0031	–36.02	–6.022	0.0623
13	31	0.8653	3.074		2.084	1.734	
14	41	–1.172	4.900		–1.735	2.490	
23	32	91.66	–37.46		–3.963	–40.65	
24	42	–1.875	7412		–5.326	–27.18	
34	43	1.107	1.479		0.9353	7.457	
313.15 K							
12	21	–41.39	–1.595	0.0033	–12.47	3.027	0.0967
13	31	1.031	3.053		1.123	4.229	
14	41	–1.181	2.445		0.5545	0.2949	
23	32	–2.091	–39.16		2.319	–19.22	
24	42	–2.079	7411		30.16	–5.590	
34	43	1.272	2.137		2.146	1.796	

Table 11. NRTL and UNIQUAC Interaction Parameters for *N*-Heptane (1) + (NMP (2) + 50% Glycerol (3)) + Toluene (4) System at 298.15 and 313.15 K and 101.3 kPa

Component		NRTL Parameters ($\alpha = 0.2$)			UNIQUAC Parameters		
<i>ij</i>	<i>ji</i>	g_{ij} – g_{jj}	g_{ji} – g_{ii}	rmsd	u_{ij} – u_{jj}	u_{ji} – u_{ii}	rmsd
298.15 K							
12	21	–15.23	–2.217	0.0044	–8.615	–1.376	0.0104
13	31	2.485	1.078		6.499	1.400	
14	41	–1.150	3.607		–0.9841	6.790	
23	32	–3.611	–18.24		–3.056	57.94	
24	42	–2.430	–20.43		–4.665	–4.665	
34	43	2.471	8.525		2.236	12.96	
313.15 K							
12	21	–17.28	–2.025	0.0030	–18.00	5.566	0.054
13	31	0.1991	3.108		1.349	2.920	
14	41	–0.9879	2.002		–0.9821	0.6230	
23	32	–3.064	–85.58		–0.8788	–332.7	
24	42	–3.035	–18.76		–7.848	–18.13	
34	43	2.235	4.435		2.170	3.900	

NMP. A similar phenomenon is observed in the work of Brijmohan et al.⁴⁵ The sharp decrease in selectivity observed with pure NMP is less pronounced in the NMP + 10% glycerol, NMP + 30% glycerol, and NMP + 50% glycerol systems, suggesting that the improved selectivity can be attributed to glycerol in the solvent mixtures. A similar observation can be drawn from the work of Brijmohan et al.⁴⁵ This improvement in selectivity is in the order: NMP + 50% glycerol > NMP + 30% glycerol > NMP + 10% glycerol. Although the selectivity has shown an improvement, conventional solvents still have superior selectivities. The solvents under investigation showed good capacities, especially NMP + 50% glycerol. These findings were outside the scope of the initial predictions, as the poor capacities associated with glycerol were expected to carry over with an increase in glycerol content. According to Green and Southard,⁴⁸ a relatively large two-phase region is indicative of the magnitude of the solvent capacity. Hence, the NMP + 50% glycerol system, having the largest two-phase region, demonstrated this.

**Figure 8.** Selectivity comparison with respect to toluene content in the *n*-heptane-rich phase for the system *n*-heptane (1) + solvent (2) + toluene (3) at 298.15 K and 101.3 kPa. Solvents: ■, pure glycerol; –, pure NMP; ○, NMP + 10% glycerol; ×, NMP + 30% glycerol; ●, NMP + 50% glycerol; ▲, sulfolane; ◆, NFM.**Figure 9.** Selectivity comparison with respect to toluene content in the *n*-heptane-rich phase for the system *n*-heptane (1) + solvent (2) + toluene (3) at 313.15 K and 101.3 kPa. Solvents: ■, pure glycerol; –, pure NMP; ○, NMP + 10% glycerol; ×, NMP + 30% glycerol; ●, NMP + 50% glycerol; ▲, sulfolane; ◆, NFM.

Furthermore, the good capacities demonstrated by the solvents under investigation can be attributed to the very high capacities associated with pure NMP.⁴⁹ Saha et al.,⁵⁰ observed a similar trend and reported higher capacities for toluene recovery using a solvent mixture of NMP and tetraethylene glycol compared to the use of pure tetraethylene glycol. The changes in the extent of the two-phase region at increased temperatures are evident in the capacity, as shown in Figures 10 and 11, suggesting that there was a slight decrease in this region. At 313.15 K, the solubility of toluene in the solvent mixtures is higher than the solubility of *n*-heptane in the solvent mixtures. Overall, a trade-off between a high selectivity and a low capacity versus a low selectivity and a high capacity is seen among all solvents at both temperatures.

As previously mentioned, the properties that govern solvent selection are high selectivity for aromatics, high capacity, the ability to form two phases at reasonable temperatures, and low risks to health, safety, and the environment (HSE). NMP + 50% glycerol demonstrated the best selectivity with increasing

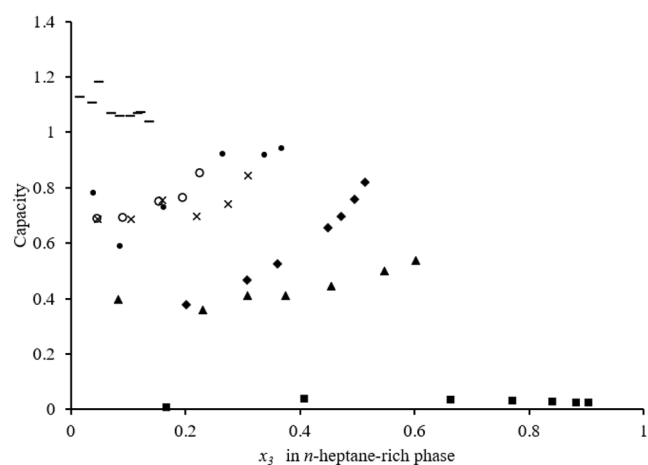


Figure 10. Capacity comparison with respect to toluene content in the *n*-heptane-rich phase for the system *n*-heptane (1) + solvent (2) + toluene (3) at 298.15 K and 101.3 kPa. Solvents: ■, pure glycerol; -, pure NMP; ○, NMP + 10% glycerol; ×, NMP + 30% glycerol; ●, NMP + 50% glycerol; ▲, sulfolane; ◆, NFM.

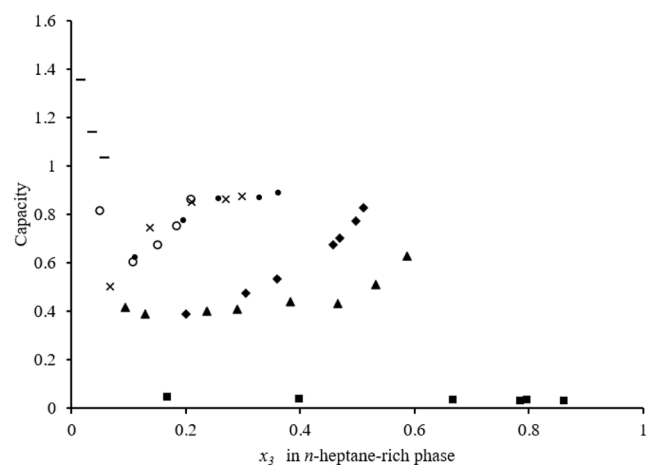


Figure 11. Capacity comparison with respect to toluene content in the *n*-heptane-rich phase for the system *n*-heptane (1) + solvent (2) + toluene (3) at 313.15 K and 101.3 kPa. Solvents: ■, pure glycerol; -, pure NMP; ○, NMP + 10% glycerol; ×, NMP + 30% glycerol; ●, NMP + 50% glycerol; ▲, sulfolane; ◆, NFM.

aromatic content in the feed. This would mean that its application could lead to reduced capital costs due to the high selectivity and the absence of additional equipment needed to recover glycerol's negligible losses.^{18,19} NMP + 50% glycerol also demonstrated the largest area for separation and the best capacity at low temperatures. However, these capacities are not comparable to those of conventional solvents. Therefore, the use of the solvents investigated could be accompanied by high solvent-to-feed ratios. NMP + 50% glycerol system contained more glycerol, which encourages the use of greener solvents. However, its application might not be practical on an industrial scale due to the high viscosities associated with glycerol. Glycerol has a viscosity of approximately 582.60 mPa·s, which is large compared to conventional solvents.¹⁸ The high viscosity of glycerol reduces the solubility and molecular transfer of solutes in the solvent-rich phase, thereby requiring high energy consumption and pumping costs.⁵¹ This effect can be mitigated by reducing the amount of glycerol and avoiding it as a major constituent of the solvent. However, this comes at

the expense of reducing other desired properties. Therefore, among the solvents investigated, the most suitable solvent would be a trade-off between these properties.

4. CONCLUSION

This investigation focused on identifying solvent mixtures of NMP and glycerol as alternatives in aromatic recovery to encourage the use of greener solvents. This was done by the effective separation of toluene from *n*-heptane using solvent mixtures of NMP and glycerol, with ratios of NMP to glycerol at 90:10, 70:30, and 50:50. New LLE data were measured for systems *n*-heptane + the solvent mixture + toluene at 298.15 and 313.15 K and 101.3 kPa using the direct analytical technique. The LLE data were found to be better correlated with the β function equation and the NRTL activity coefficient model. All systems exhibited type I ternary LLE behavior. The selectivity was greater than unity across all systems and temperatures, indicating an effective separation. The systems demonstrated improved selectivities and capacities with an increase in glycerol. Therefore, the selection of the ideal solvent would be a trade-off between solvent performance, process design, impact on HSE, and capital and operational costs.

■ AUTHOR INFORMATION

Corresponding Author

Naadhira Seedat – Department of Chemical Engineering, Faculty of Engineering and the Built Environment, University of Johannesburg, Doornfontein 2028, South Africa; Department of Chemical Engineering, University of Pretoria, Pretoria 0028, South Africa; orcid.org/0000-0001-8745-1127; Email: naadhira.seedat@up.ac.za

Authors

Blessing Mcebo Paile – Department of Chemical Engineering, Faculty of Engineering and the Built Environment, University of Johannesburg, Doornfontein 2028, South Africa
Caleb Narasigadu – School of Chemical and Minerals Engineering, Faculty of Engineering, Potchefstroom Campus, North-West University, Potchefstroom 2351, South Africa; orcid.org/0000-0001-9224-136X

Complete contact information is available at: <https://pubs.acs.org/10.1021/acs.jced.4c00614>

Funding

B.P.: Conceptualization, formal analysis, investigation, writing – original draft. C. N.: Conceptualization, supervision, resources, methodology, writing – reviewing and editing. N.S.: Supervision, resources, project administration, writing – reviewing and editing.

Notes

The authors declare no competing financial interest.

■ ACKNOWLEDGMENTS

This work is based upon research supported by the National Research Foundation of South Africa.

■ REFERENCES

- (1) Wang, H.; Liu, W.; Shi, F.; Huang, L.; Lian, J.; Qu, L.; Cai, J.; Xu, Z. Metabolic pathway engineering for high-level production of 5-hydroxytryptophan in *Escherichia coli*. *Metab. Eng.* **2018**, *48*, 279–287.
- (2) Aversch, N. J. H.; Kromer, J. O. Metabolic Engineering of the Shikimate Pathway for Production of Aromatics and Derived

Compounds—Present and Future Strain Construction Strategies. *Front. Bioeng. Biotechnol.* **2018**, *6*, 32.

(3) Nekhaev, A. I.; Maksimov, A. L. Production of Aromatic Hydrocarbons from Biomass. *Pet. Chem.* **2021**, *61* (1), 15–34.

(4) Brijmohan, N.; Narasigadu, C. Ternary Liquid–Liquid Equilibrium Data for the N-Formylmorpholine + Toluene + {n-Nonane or n-Decane} Systems at (303.2, 323.2, and 343.2) K and 101.3 kPa. *J. Chem. Eng. Data* **2020**, *65* (2), 788–792.

(5) Franck, H.-G.; Stadelhofer, J. W. *Industrial Aromatic Chemistry: raw Materials · Processes · Products*; Springer Science & Business Media, 2012.

(6) Meindersma, G. W.; de Haan, A. B. Conceptual process design for aromatic/aliphatic separation with ionic liquids. *Chem. Eng. Res. Des.* **2008**, *86*, 745–752.

(7) Díaz, I.; Palomar, J.; Rodríguez, M.; De Riva, J.; Ferro, V.; González, E. J. Ionic liquids as entrainers for the separation of aromatic–aliphatic hydrocarbon mixtures by extractive distillation. *Chem. Eng. Res. Des.* **2016**, *115*, 382–393.

(8) Seddon, K. R. Ionic liquids for clean technology. *J. Chem. Technol. Biotechnol.* **1997**, *68* (4), 351–356.

(9) Canales, R. I.; Brennecke, J. F. Comparison of Ionic Liquids to Conventional Organic Solvents for Extraction of Aromatics from Aliphatics. *J. Chem. Eng. Data* **2016**, *61* (5), 1685–1699.

(10) Alkhalidi, K. H. A. E.; Fandary, M. S.; Al-Jimaz, A. S.; Al-Tuwaim, M. S.; Fahim, M. A. Liquid–liquid equilibria of aromatics removal from middle distillate using NMP. *Fluid Phase Equilib.* **2009**, *286* (2), 190–195.

(11) Meindersma, G. W.; Podt, A. J. G.; de Haan, A. B. Ternary liquid–liquid equilibria for mixtures of toluene+n-heptane+an ionic liquid. *Fluid Phase Equilib.* **2006**, *247* (1–2), 158–168.

(12) DongChu, C.; HongQi, Y.; Hao, W. (Liquid+ liquid) equilibria of {heptane+ xylene+ N-formylmorpholine} ternary system. *J. Chem. Thermodyn.* **2007**, *39* (12), 1571–1577.

(13) Mohsen-Nia, M.; Modarress, H.; Doulabi, F.; Bagheri, H. Liquid + liquid equilibria for ternary mixtures of (solvent + aromatic hydrocarbon + alkane). *J. Chem. Thermodyn.* **2005**, *37* (10), 1111–1118.

(14) Mesquita, F. M. R.; Pinheiro, R. S.; Santiago-Aguiar, R. S.; de Sant'ana, H. B. Measurement of phase equilibria data for the extraction of toluene from alkane using different solvents. *Fluid Phase Equilib.* **2015**, *404*, 49–54.

(15) Saha, M.; Rawat, B.; Khanna, M.; Nautiyal, B. Liquid– liquid equilibrium studies on toluene+ heptane+ solvent. *J. Chem. Eng. Data* **1998**, *43* (3), 422–426.

(16) Reddy, P.; Letcher, T. M. Chapter 5 - Phase Equilibrium Studies on Ionic Liquid Systems for Industrial Separation Processes of Complex Organic Mixtures. In *Thermodynamics, Solubility and Environmental Issues*; Letcher, T. M. Ed.; Elsevier, 2007, pp. 85–111.

(17) Mueller, E.; Hochfield, G. Aromatics Extraction with Solvent Combinations. In *7th World Petroleum Congress*; OnePetro, 1967.

(18) Brijmohan, N.; Moodley, K.; Narasigadu, C. Identification and Screening of Potential Organic Solvents for the Liquid–Liquid Extraction of Aromatics. *Org. Process Res. Dev.* **2021**, *25* (10), 2230–2248.

(19) Brijmohan, N.; Moodley, K.; Narasigadu, C. Ternary Liquid–Liquid Equilibrium Data for the n-Heptane+ Toluene+(Butane-1, 4-diol or Glycerol) Systems at 298.2, 313.2, and 333.2 K and 0.1 MPa. *J. Chem. Eng. Data* **2022**, *67* (4), 975–983.

(20) Taylor, B. N.; Kuyatt, C. E. *Guidelines for evaluating and expressing the uncertainty of NIST measurement results*; US Department of Commerce, Technology Administration, National Institute of Standards and Technology, 1994.

(21) O'Neil, M. J. *The Merck index: an encyclopedia of chemicals, drugs, and biologicals*; RSC Publishing, 2013.

(22) Haynes, W. M. *CRC handbook of chemistry and physics*; CRC press, 2016.

(23) Alders, L. *Liquid-liquid extraction: theory and laboratory practice*; Elsevier Publishing Company, 1959.

(24) Narasigadu, C.; Naidoo, M.; Ramjugernath, D. Ternary Liquid–Liquid Equilibrium Data for the Water + Acetonitrile + {Butan-1-ol or 2-Methylpropan-1-ol} Systems at (303.2, 323.2, 343.2) K and 1 atm. *J. Chem. Eng. Data* **2014**, *59* (11), 3820–3824.

(25) Mühlbauer, A. L.; Raal, J. D.; *Phase equilibria: Measurement and computation*; Taylor & Francis, 1998.

(26) Box, G. E. P.; Hunter, J. S.; Hunter, W. G. *Statistics for experimenters: Design, innovation, and discovery*; Wiley-Interscience, 2005.

(27) Bulatov, S. N.; Yachmenev, L. T. Approximation of binodal curves of heterogeneous ternary systems. *Teor. Osn. Khim. Technol.* **1971**, *5*, 644–650.

(28) Hlavatý, K. Correlation of the binodal curve in a ternary liquid mixture with one pair of immiscible liquids. *Collect. Czech. Chem. Commun.* **1972**, *37* (12), 4005–4007.

(29) Letcher, T. M.; Heyward, C.; Wootton, S. Phase separation in petrol-alcohol blends. *S. Afr. J. Chem.* **1986**, *39* (1), 19–22.

(30) Letcher, T. M.; Siswana, P. M.; Van Der Watt, P.; Radloff, S. Phase equilibria for (an alkanol + p-xylene + water) at 298.2 K. *J. Chem. Thermodyn.* **1989**, *21* (10), 1053–1060.

(31) Procházka, J.; Heyberger, A. Correlation of ternary liquid-liquid equilibria in system isobutyl acetate-acetic acid-water. *Chem. Eng. Sci.* **1996**, *51* (6), 893–903.

(32) Olán-Acosta, M. D. L. Á.; Castrejón-González, E. O.; Alvarado, J. F. J.; Rico-Ramírez, V. Approximate design method for reactive liquid extractors based on thermodynamic equilibrium correlations. *Chem. Eng. Res. Des.* **2016**, *109*, 443–454.

(33) Narasigadu, C.; Raal, J. D.; Naidoo, P.; Ramjugernath, D. Ternary liquid– liquid equilibria of acetonitrile and water with heptanoic acid and nonanol at 323.15 K and 1 atm. *J. Chem. Eng. Data* **2009**, *54* (3), 735–738.

(34) Naidoo, R. D.; Letcher, T. M.; Ramjugernath, D. Ternary Liquid–Liquid Equilibria for Pseudoternary Mixtures Containing an n-Alkane + an Aromatic Hydrocarbon + {N-Methyl-2-pyrrolidinone + a Solvent} at 298.2 K and 1 atm. *J. Chem. Eng. Data* **2001**, *46* (6), 1375–1380.

(35) Sen, A.; Srivastava, M. *Regression Analysis: theory, Methods, and Applications*; Springer: New York, 1990.

(36) Renon, H.; Prausnitz, J. M. Local compositions in thermodynamic excess functions for liquid mixtures. *Aiche J.* **1968**, *14* (1), 135–144.

(37) Anderson, T. F.; Prausnitz, J. M. Application of the UNIQUAC equation to calculation of multicomponent phase equilibria. I. Vapor-liquid equilibria. *Ind. Eng. Chem. Process Des. Dev.* **1978**, *17* (4), 552–561.

(38) Britt, H. I.; Luecke, R. H. The estimation of parameters in nonlinear, implicit models. *Technometrics* **1973**, *15* (2), 233–247.

(39) Deming, W. E. *Statistical adjustment of data*; John Wiley & Sons, 1943.

(40) Novák, J. P.; Matouš, J.; Pick, J. *Liquid-liquid Equilibria*; Elsevier, 1987.

(41) Walas, S. M. *Phase equilibria in chemical engineering*; Butterworth, 1985.

(42) DongChu, C.; HongQi, Y.; Hao, W. (Liquid+ liquid) equilibria of three ternary systems: (heptane+ benzene+ N-formylmorpholine), (heptane+ toluene+ N-formylmorpholine), (heptane+ xylene+ N-formylmorpholine) from T = (298.15 to 353.15) K. *J. Chem. Thermodyn.* **2007**, *39* (8), 1182–1188.

(43) Coolidge, A. S. Phase equilibria for three component systems containing two liquid phases, the complete composition of at least one of which is known. *International Critical Tables Of Numerical Data, Physics, Chemistry And Technology*; McGraw-Hill: New York, 1928; 398–417.

(44) Treybal, R. E. *Liquid extraction*; McGraw-Hill, 1963.

(45) Brijmohan, N.; Moodley, K.; Narasigadu, C. Use of Glycerol + 2-Methylpentane-2,4-diol Liquid Mixtures in the Separation of Toluene from n-Heptane via Liquid–Liquid Extraction. *J. Chem. Eng. Data* **2023**, *68* (11), 2934–2945.

(46) Ferreira, P. O.; Ferreira, J. B.; Medina, A. G. Liquid-liquid equilibria for the system N-methylpyrrolidone + toluene + n-heptane: UNIFAC interaction parameters for N-methylpyrrolidone. *Fluid Phase Equilib* **1984**, *16* (3), 369–379.

(47) Tripathi, R. P.; Ram, A. R.; Rao, P. B. Liquid-liquid equilibria in ternary system toluene-n-heptane-sulfolane. *J. Chem. Eng. Data* **1975**, *20* (3), 261–264.

(48) Green, D. W.; Southard, M. Z. *Perry's Chemical Engineers' Handbook*; McGraw-Hill Education, 2019.

(49) Nagpal, J. M.; Rawat, B. S. Liquid-liquid equilibria for toluene-heptane-N-methyl pyrrolidone and benzene-heptane solvents. *J. Chem. Technol. Biotechnol.* **1981**, *31* (1), 146–150.

(50) Saha, M.; Rawat, B. S.; Khanna, M. K.; Nautiyal, B. R. Liquid-Liquid Equilibrium Studies on Toluene + Heptane + Solvent. *J. Chem. Eng. Data* **1998**, *43* (3), 422–426.

(51) Kislik, V. S. Chapter 13 - Advances in Development of Solvents for Liquid-Liquid Extraction. In *Solvent Extraction*; Kislik, V. S. Ed.; Elsevier, 2012. pp. 451–481.



CAS BIOFINDER DISCOVERY PLATFORM™

**PRECISION DATA
FOR FASTER
DRUG
DISCOVERY**

CAS BioFinder helps you identify
targets, biomarkers, and pathways

Unlock insights

CAS
A division of the
American Chemical Society